Electronic Supplementary Material

Rational Design of a "Dual Lock-and-Key" Supramolecular Photosensitizer Based on Aromatic Nucleophilic Substitution for Specific and Enhanced Photodynamic Therapy

Kun-Xu Teng, Li-Ya Niu*, Yan-Fei Kang, and Qing-Zheng Yang*

Key Laboratory of Radiopharmaceuticals, Ministry of Education, College of Chemistry, Beijing Normal University, Beijing 100875, P. R. China.
Email: niuly@bnu.edu.cn, qzyang@bnu.edu.cn

1. General information

1.1 Materials and Instruments.

Unless otherwise mentioned, materials were obtained from commercial suppliers and were used without further purification. All reactions were performed in oven-dried glasswares (Hinwil) unless otherwise stated. PEG_{5000}-PAE_{10000} and PCL_{10000}-PEG_{5000} were purchased from Xi'an ruixi Biotechnology Co., Ltd (XI'an, China). Column chromatography was performed over silica gel (200-300 mesh). NMR spectra were recorded with JEOL-400 or JEOL-600 spectrometers. High-resolution mass spectrometry experiments were recorded by Bruker Solarix XR Fourier Transform Ion Cyclotron Resonance Mass Spectrometer. All optical spectra were recorded at room temperature. Absorption spectra of liquid samples were determined on Hitachi UV-3900 spectrophotometer. Fluorescence spectra of liquid samples were determined on Hitachi F-4600 spectrophotometer. Fluorescence lifetime of liquid samples were determined on Edinburgh FLS 980 spectrometer. Dynamic light scattering (DLS) investigations were carried out with a DynaPro NanoStar dynamic light scattering detector. Transmission electron microscope (TEM) images were obtained using a FEI Talos F200S instrument. The Zeta-potential was obtained using 90 plus zeta (Brookhaven) instrument. The photostability was conducted under irradiation with a Xenon lamp without a filter and monitored using an UV-3900 spectrophotometer. Single-particle imaging were performed on a wide-field setup based on an inverted Nikon Eclipse Ti microscope (Nikon nstruments) with the Perfect Focus System, applying objective-type total internal reflection fluorescence (TIRF) mode with a high-numerical aperture (NA) TIRF objective (SR Apo TIRF 60×, Oil, NA 1.49). Irradiation was performed using a LED light (PLS-LED 100, Perfect Light, Beijing, China). Flow cytometry test of apoptosis were carried out with a CytoFLEX (BECKMAN) instrument. In vivo imaging was recorded using an IVIS Spectrum imaging system (PerkinElmer, USA). The histopathological photos of the tissues were obtained by using a digital slide scanner (Pannoramic DESK, P-MIDI, P250, P1000). BALB/c nude mice and tumor-bearing mouse model were purchased from Beijing Vital River Laboratory Animal Technology Co. Ltd. All animal experiments were completed under the guidance of the Key Laboratory of Radiopharmaceuticals of Beijing Normal University.

1.2 Detection the critical micelle concentration (CMC)

CMC of PEG_{5000}-PAE_{10000} was determined by fluorescence with Nile Red as the probe of polarity. Aqueous solutions of PEG_{5000}-PAE_{10000} at different concentrations (10 μg/mL, 20 μg/mL, 30 μg/mL, 50 μg/mL, 100 μg/mL, 150 μg/mL, 200 μg/mL, 300 μg/mL, 400 μg/mL) were prepared, as well as a 1 mM solution of Nile Red in THF. To each of the solutions of PEG_{5000}-PAE_{10000} (2.0 mL), 10 μL solution of Nile Red was added. The solutions were then sonicated for 60 min and the fluorescence spectra of the resulting solutions were recorded. The value of fluorescence intensity was plotted as a function of the concentration of PEG_{5000}-PAE_{10000} (Fig. S4).

1.3 Detection of $^1O_2$ production in solution.

In this experiment, 15 μM of BIBCl-PAE NPs with GSH (1 mM) and BIBCl-PAE NPs without GSH, as well as Ce6 were suspended in 2 mL buffer containing 20 μM of ABDA, which is a singlet oxygen inductor. The mixture was then placed in a cuvette and irradiated with a white LED light source at 10 mW cm^{-2} for 4 minutes. The absorption changes of ABDA (at 378 nm) was measured using a UV-Vis absorption spectrophotometer.

BIBSG, BIBCl, BI and BSG were measured in DMF under the same conditions.

1.4 Cell Culture and Cellular uptake.

Cells were cultured in culture media (DMEM/F12 supplemented with 10% FBS, 50 U/mL penicillin, and 50 μg mL^{-1} streptomycin) at 37 °C in a humidified atmosphere of 5% CO_2 and 95% air for 24 h. For fluorescence imaging, the cells were incubated with 2.5 μg mL^{-1} BIBCl-PAE NPs at 37 °C for different time and then washed with 1× phosphate-bu□ered saline (PBS) three times. Confocal fluorescence imaging was performed with Nikon single-particle microscopy with a 60 × oil-immersion objective lens.

1.5 In vitro PDT.

HepG2 cells (the same method for Hela, A549 and L02 cells) were seeded in 96-well plates (5×10^3 cells $well^{-1}$) and incubated for 24 hours. Then, the medium was replaced with 100 μL of DMEM containing different concentrations of nano drug. After incubation for another 12 hours, the cells were washed three times with PBS, infused with fresh medium, and illuminated by a white LED light (50 mW cm^{-2}, 400-800 nm) for 10 min. After further incubation for 24 h, the cell viability was examined by cell counting kit-8 (CCK-8) assays. Moreover, the dark toxicity of the samples was analysed using the above procedure except the illumination was eliminated.

1.6 Singlet oxygen generation in living cells.

$^1O_2$ generated in cells treated with PDT were detected using reactive oxygen species indictors immediately after the photosensitization experiments. Specifically, the HepG2 cells were incubated with 2.5 μg mL^{-1} BIBCl-PAE NPs at 37 °C under 5% CO_2 for 12 hours and then washed with PBS three times. The culture medium was replaced with DMEM containing 5 μM 2′ ,7′ -dichlorofluorescein-diacetate (DCFH-DA) that sufficiently covered the adhering cells and the cells were then subjected to the photosensitization experiment with white LED irradiations for 10 min. After that, the DMEM was removed and the remaining DCFH-DA was washed with PBS buffer three times. Fluorescent images of DCFH-DA, staining on the cells were promptly captured by Nikon single-particle microscopy with a 60 × oil-immersion objective lens. Singlet oxygen sensor green reagent (SOSG) staining was carried out in the same method as DCFH-DA.

1.7 Calcein AM/PI staining of HepG2 cells in PDT experiments.

The HepG2 cells were seeded on 35 mm confocal dishes and incubated for 24 h. The medium was then replaced with fresh culture medium containing BIBCl-PAE NPs (5.0 μg/mL) and incubated for 12 h. Then, the cells were irradiated with a white LED light (20 mW cm^{-2}, 400-800 nm) for 5 min. After further incubation for 5 h, the cells were stained with Calcein AM and propidium iodide (PI). After 15 min, the calcein AM and PI solution was removed and washed with PBS buffer three times. Fluorescent images of Calcein AM and PI, staining on the

cells were promptly captured by Nikon single-particle microscopy with a 60 × oil-immersion objective lens.

1.8 Flow Cytometry Test of Apoptosis.

The HepG2 cells were seeded on 6 well cell culture plate and incubated for 24 h. The medium was then replaced with fresh culture medium containing BIBCl-PAE NPs (5.0 μg/mL) and incubated for 12 h. Then, the cells were irradiated with a white LED light (20 mW cm^{-2}, 400-800 nm) for 30 min. After further incubation for 12 h, the cells were collected and treated with AnnexinV-FITC/PI cell apoptosis detection kit. The flow cytometry was used to detect cell apoptosis. This experiment was performed by Yimingtongchuang Biological Technology Co., Ltd.

1.9 Targeted PDT on subcutaneous HepG2 tumor model.

Tumor targeting property of BIBCl-PAE NPs were studied with subcutaneous tumor model of human liver cancer HepG2 in the immunocompetent BALB/c mice. The tumor-bearing mice were intravenously injected at the dose of 2 mg kg^{-1} BIBCl. Then, we measured the fluorescence at different time points (0 (before inject), 3, 6, 9, 12, 24 hours) with an IVIS Spectrum imaging system (PerkinElmer, USA). The excitation wavelength was 675 nm and the emission wavelength was 720 nm.

1.10 In vivo Biodistribution of BIBCl-PAE NPs.

The ex vivo biodistribution of photosensitizer was evaluated at 24 hours postinjection by IVIS Spectrum imaging. Mice were sacrificed and their major organs including heart, liver, spleen, lung, kidney, pancreas, stomach, intestines and tumor were carefully removed for visualization under the imaging system.

1.11 In vivo PDT experiment.

Phototoxicity assay was performed using HepG2 tumor bearing mice. The mice were divided into five different groups for treatment: Group 1: PBS injection with irradiation; Group 2: BIBCl-PAE NPs injection without irradiation; Group 3: BIBCl-PCL NPs injection with irradiation; Group 4: BIBH-PAE NPs injection with irradiation; Group 5: BIBCl-PAE NPs with irradiation. Each group contained five mice. Nanomicelle (250 μg mL^{-1}, 100 μL) in PBS was injected via tail vein. 9 h later and 24 h later, white light LED (100 mW cm^{-2}, 400-800 nm) treatment was performed on groups 1, 3, 4, 5 by irradiating the tumor region for 30 min. The effect of the different treatment groups was monitored by measuring tumor size (tumor size = width × width × length/ 2.) and mice body weight 14 days after PDT treatment. After 14 days, the tumors were dissected and weighed. Tumor tissues of the abovementioned treatment groups 1−5 were harvested for histological study by hematoxylin-eosin (H&E) staining under a digital slide scanner. The fixation of tissues and H&E staining were performed by servicebio Co., Ltd.

1.12 Histology

The subcutaneous HepG2 tumor-bearing mice were treated with BIBCl-PAE NPs through intravenouse injection from the tail vein (250 μg mL^{-1}, 100 μL). After injection 9 h, the tumor region of mice was irradiated by white LED (100 mW cm^{-2}, 400-800 nm) for 30 min. Set the non-illuminated group as a control. On the third day, tissues including liver, spleen, kidney,

heart, lung and paracancerous tissue were harvested, fixed in paraffin, and sectioned for H&E staining. The histopathological photos of the tissues were obtained by using a digital slide scanner. The fixation of tissues and H&E staining were performed by servicebio Co., Ltd.

2. Molecules synthesis and preparation of nanoparticles

1) Synthesis of **BCl**

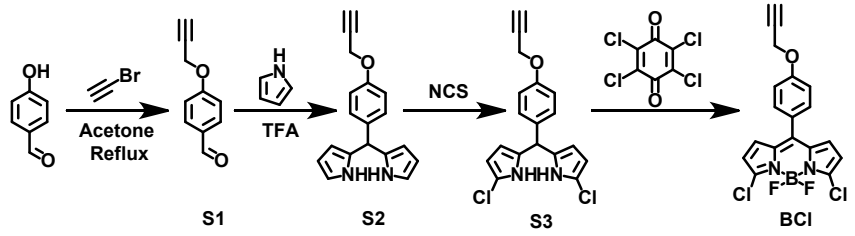

Scheme S1 Synthesis of **BCl.**

Synthesis of **S1**: To the 500 mL round-bottom flask were added p-Hydroxybenzaldehyde (2.44 g, 20 mmol), propargyl bromide (1.49 ml, 20 mmol), K_2CO_3 (2.76 g, 20 mmol) and acetone (80 mL), and then the reaction mixture was refluxed for 12 hours. The reaction was monitored by TLC and the result indicated that the raw material disappeared and new products were formed. K_2CO_3 was removed by filtration. Monomer 1.00 g was recrystallized from acetone. Yield: 98%.

Synthesis of **S2**: 5 mL 36% HCl was dispersed into 100 mL distilled water under stirring. Pyrrole (2.7 mL, 38.6 mmol) was added into the solution and stirred for 0.5 hour at room temperature. **S1** (1g, 6.24 mmol) was added into the reaction mixture under rapid stirring. After reaction for 1 hour at room temperature, 2 mL NH_3•H_2O was added into the solution to quench the reaction. Then, 50 mL dichloromethane was added to the resulting mixture and the product was extracted into the organic phase. The product was extracted with dichloromethane (3 × 50 mL) and the organic layers were combined. The organic solution was dried over anhydrous sodium sulfate and evaporated under reduced pressure. The crude product (0.88 g) was directly used for the next step without purification.

Synthesis of **BCl**: A solution of compound **S2** (0.83 g, 3.0 mmol) in THF (60 mL) was cooled to -78 °C. N-Chlorosuccinimide (0.40 g, 3.0 mmol) in THF (50 mL) was added via dropping funnel over the course of 1 hour. The reaction was stirred for an additional 1 hour to room temperature. Then, the resulting solution was concentrated, and the residue was diluted with dichloromethane (80 mL), followed by washing with saturated saline (2 × 80 mL). The organic layers were collected, dried over anhydrous Na_2SO_4 and concentrated under reduced pressure. The crude product **S3** was directly used for the next step without purification. Chloranil (439 mg, 1.78 mmol) in dichloromethane (10 mL) was added dropwise to the solution of compound **S3** in dichloromethane (80 mL). After the resulting mixture was stirred for 1 hour at room temperature, Et_3N (1.6 mL, 11.3 mmol) was added to the reaction mixture. The resulting mixture was stirred for an additional 0.5 hour at room temperature, followed by adding BF_3•OEt_2 (2.81 mL, 22.6 mmol) via syringe. After stirring in the dark for 3 hours at room temperature, water (90 mL) was added to the solution, and the organic layers was collected,

washed with water, dried over anhydrous Na_2SO_4, and concentrated under vacuum. Purification by column chromatography on silica gel with petroleum ether/dichloromethane (60/40 v/v) afforded **BCl** (210 mg, 17.9 %) as red solid. ^{1}H NMR (400 MHz, Chloroform-*d*) δ 7.46 (d, *J* = 8.4 Hz, 1H), 7.12 (d, *J* = 8.3 Hz, 1H), 6.88 (d, *J* = 3.8 Hz, 1H), 6.47 – 6.41 (m, 196H), 4.79 (s, 1H), 2.60 (s, 1H).

2) Synthesis of **BI**

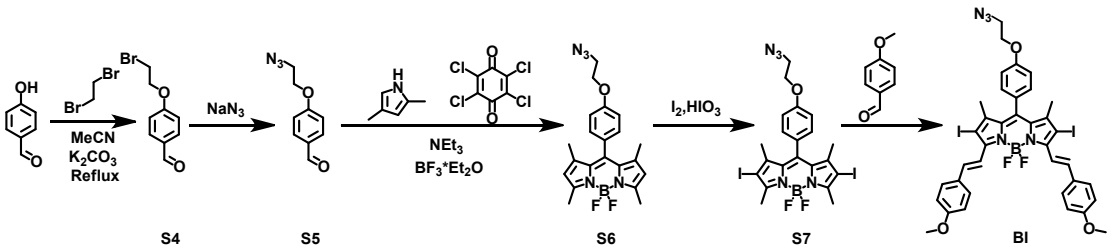

Scheme S2 Synthesis of **BI.**

The synthesis of S4-S7 refers to the reported method.[1]

Synthesis of **BI**: Compound S7 (920 mg, 1.4 mmol), p-methoxybenzaldehyde (413.7 mg, 3.0 mmol), piperidine (5 mL) and glacial acetic acid (5 mL) were mixed in benzene (35 mL) under N_2 atmosphere and heated under reflux for 12 hours. Then, the solvent was removed under reduced pressure and the residue was purified by column chromatography on silica gel with ethyl acetate/dichloromethane (10:90, v/v) as eluent, green solid compound **BI** was obtained (264 mg, 21 %). ^{1}H NMR (600 MHz, Chloroform-*d*) δ 8.14 (d, *J* = 16.6 Hz, 1H), 7.64 – 7.57 (m, 4H), 7.20 (d, *J* = 8.6 Hz, 1H), 7.07 (d, *J* = 8.5 Hz, 1H), 6.96 (d, *J* = 8.7 Hz, 2H), 4.24 (t, *J* = 4.9 Hz, 1H), 3.90 (s, 0H), 3.87 (s, 3H), 3.69 (t, *J* = 4.9 Hz, 1H), 1.51 (s, 3H).

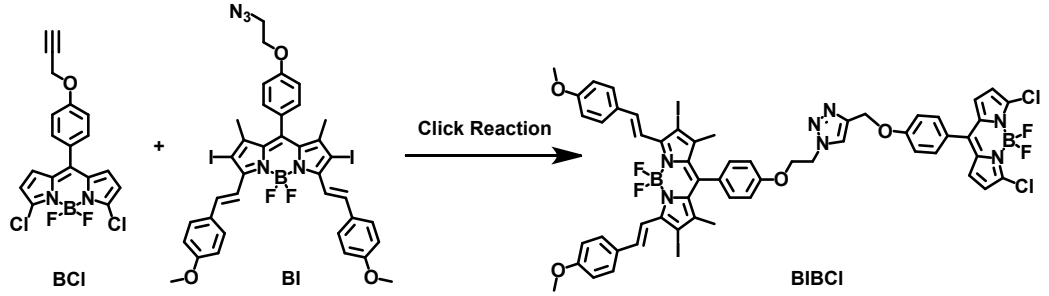

Scheme S3 Synthesis of **BIBCl.**

Synthesis of **BIBCl**: Under N_2 atmosphere, **BCl** (0.1 mmol, 39.1 mg), **BI** (0.1 mmol, 89.7 mg), $CuSO_4$•$5H_2O$ (0.01 mmol, 3.0 mg) and sodium ascorbate (0.02 mmol, 4.0 mg) were dissolved in the mixture solution ($CHCl_3$/ethanol/water, 14 mL, 12/1/1). The reaction mixture was stirred at room temperature for 24 hours. Then, the organic product was extracted into dichloromethane. The organic layer was dried over anhydrous Na_2SO_4 and evaporated to yield the crude product. The residue was purified by column chromatography on silica gel with ethyl acetate/dichloromethane (10:90, v/v) as eluent, dark green solid was obtained (97.9 mg, 76 %). ^{1}H NMR (400 MHz, Chloroform-*d*) δ 8.13 (d, *J* = 16.6 Hz, 1H), 7.91 (s, 1H), 7.59 (t, *J* = 11.3 Hz, 6H), 7.46 (d, *J* = 8.8 Hz, 2H), 7.17 (dd, *J* = 8.8, 2.2 Hz, 4H), 7.00 (d, *J* = 8.7 Hz, 2H), 6.95 (d, *J* = 8.8 Hz, 4H), 6.87 (d, *J* = 4.1 Hz, 2H), 6.43 (d, *J* = 4.3 Hz, 2H), 5.31 (s, 2H), 4.85 (t, *J* = 5.0 Hz, 2H), 4.49 (t, *J* = 5.0 Hz, 2H), 3.86 (s, 6H), 1.46 (s, 6H). ^{13}C NMR (100 MHz,

Chloroform-*d*) δ 160.90, 160.82, 158.77, 150.67, 145.51, 144.50, 143.83, 139.35, 137.82, 133.75, 133.18, 132.44, 131.48, 130.08, 129.62, 129.37, 128.68, 128.30, 128.15, 127.98, 125.52, 118.79, 116.76, 115.42, 115.05, 114.67, 114.43, 66.50, 62.19, 55.50, 17.83. HRMS: m/z; $[M]^+$, calcd for $C_{55}H_{43}O_4N_7B_2Cl_2F_4I_2^+$: 1287.0971; found: 1287.0988.

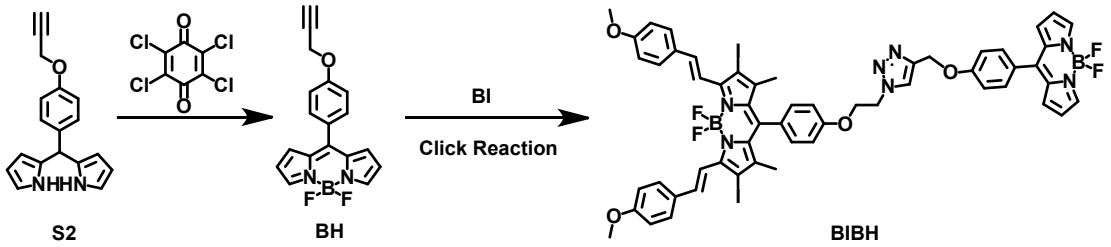

Scheme S4 Synthesis of **BIBH.**

Synthesis of **BH**: Compound **S2** (0.28 g, 1.0 mmol) was dissolved in 80 ml of dichloromethane. Then chloranil (0.50 g, 2.0 mmol) was added and stirred at room temperature for 1 hour. Triethylamine (2 mL) was added slowly and stirred for 10 min and BF_3•OEt_2 (1 mL) was added drop by drop. The reaction mixture was allowed to stirred for another 1 hour. After the reaction, the solvent was evaporated under reduced pressure. The residue was purified by column chromatography on silica gel with petroleum ether/dichloromethane (50:50, v/v) as eluent, orange solid compound **BH** was obtained (116 mg, 60 %).

Synthesis of **BIBH**: **BIBH** was prepared from **BI** and **BH** by the same method as that used to obtain **BIBCl**. ^{1}H NMR (400 MHz, Chloroform-*d*) δ 8.13 (d, *J* = 16.6 Hz, 1H), 7.97 – 7.90 (m, 8H), 7.59 (dd, *J* = 16.1, 8.8 Hz, 4H), 7.19 (dd, *J* = 8.7, 4.0 Hz, 2H), 7.02 (d, *J* = 8.7 Hz, 1H), 6.98 – 6.93 (m, 19H), 6.58 – 6.53 (m, 2H), 5.35 (s, 1H), 4.88 (t, *J* = 5.0 Hz, 1H), 4.51 (t, *J* = 4.9 Hz, 1H), 3.87 (s, 2H), 2.05 (s, 1H), 1.47 (s, 3H). ^{13}C NMR (100 MHz, Chloroform-*d*) δ 160.82, 160.72, 158.70, 150.60, 147.11, 145.48, 143.67, 143.60, 139.25, 137.78, 134.84, 133.13, 132.47, 131.34, 130.00, 129.56, 129.29, 128.59, 126.94, 124.22, 118.34, 116.71, 115.35, 114.86, 114.36, 66.42, 62.15, 55.43, 49.90, 17.76, 14.21. HRMS: m/z; $[M]^+$, calcd for $C_{55}H_{45}O_4N_7B_2F_4I_2^+$: 1219.1750; found: 1219.1750.

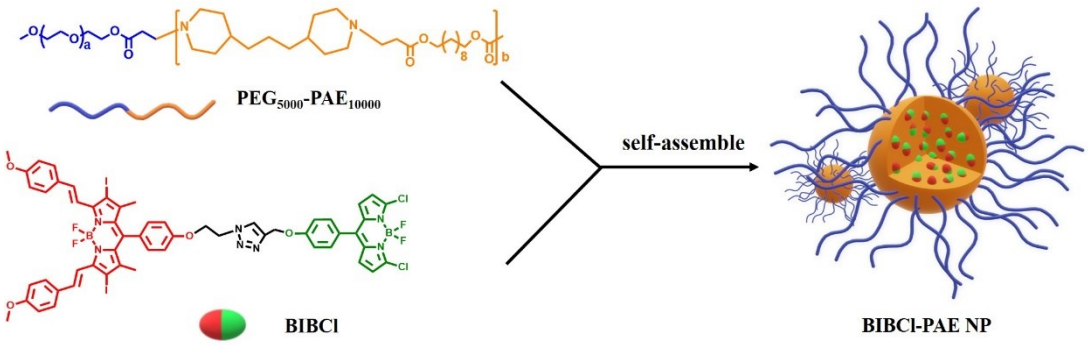

Scheme S5 Preparation of **BIBCl-PAE NPs.**

Preparation of **BIBCl-PAE NPs**: **BIBCl-PAE NPs** was prepared by self-assembly of **BIBCl** and **PEG_{5000}-PAE_{10000}** through a single-step sonication method. A 200 μL solution of **BIBCl** (1.0 mg) and **PEG_{5000}-PAE_{10000}** (4.0 mg) in THF was quickly added into 4 mL deionized water.

Then, the resulting mixture was ultrasonicated for 25 min by ultrasonic cell disruptor, centrifuged at 12000 rpm for 30 min, and washed with water to a□ord water-dispersible nanoparticles **BIBCl-PAE NPs**.

Preparation of **BIBH-PAE NPs**: **BIBH-PAE NPs** was prepared from **BIBH** and **PEG_{5000}-PAE_{10000}** by the same method as that used to obtain **BIBCl-PAE NPs**.

Preparation of **BIBCl-PCL NPs**: **BIBCl-PCL NPs** was prepared from **BIBCl** and **PEG_{5000}-PCL_{10000}** by the same method as that used to obtain **BIBCl-PAE NPs**.

Preparation of **BIBH-PCL NPs**: **BIBH-PCL NPs** was prepared from **BIBH** and **PEG_{5000}-PCL_{10000}** by the same method as that used to obtain **BIBCl-PAE NPs**.

3. Experimental data in vitro

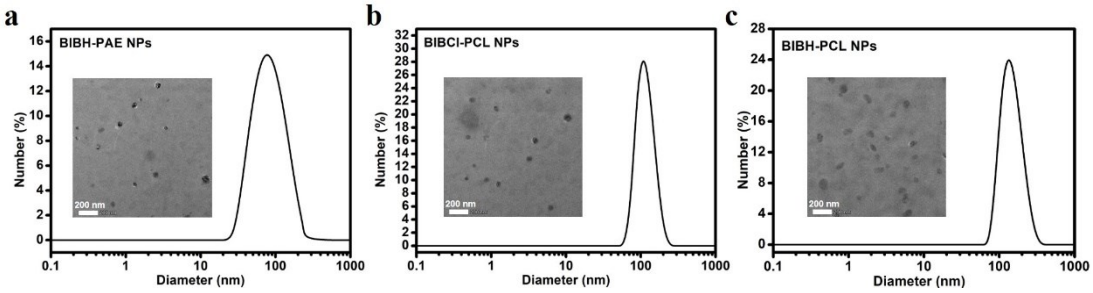

Fig. S1 DLS profiles and TEM images (inset, scale bar, 200 nm) of (a) BIBH-PAE NPs; (b)BIBCl-PCL NPs and (c) BIBH-PCL NPs.

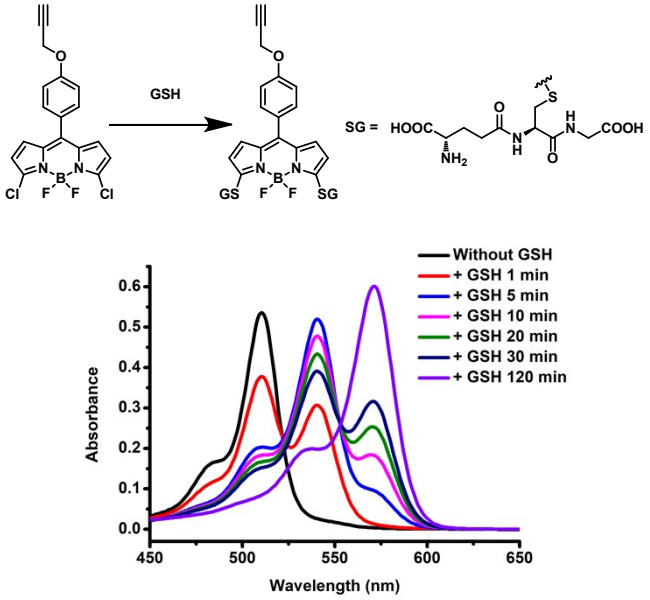

Fig. S2 Time-dependent absorption spectra of BCl (10 μM) with 100 equiv of GSH in PBS.

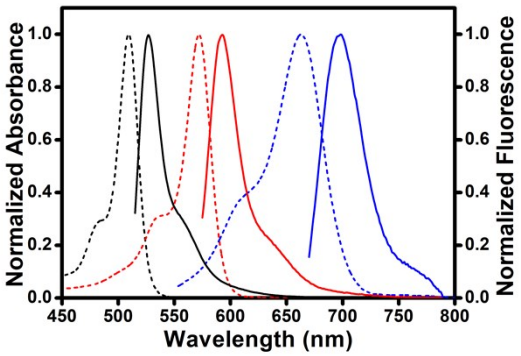

Fig. S3 Absorption spectra (dotted line) and fluorescence spectra (solid line) of BCl (black), BSG (red) and BI (blue).

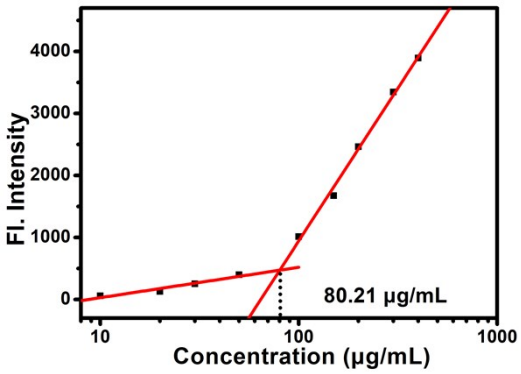

Fig. S4 Variation of fluorescence intensity of Nile Red with the concentration of PEG_{5000}-PAE_{10000}.

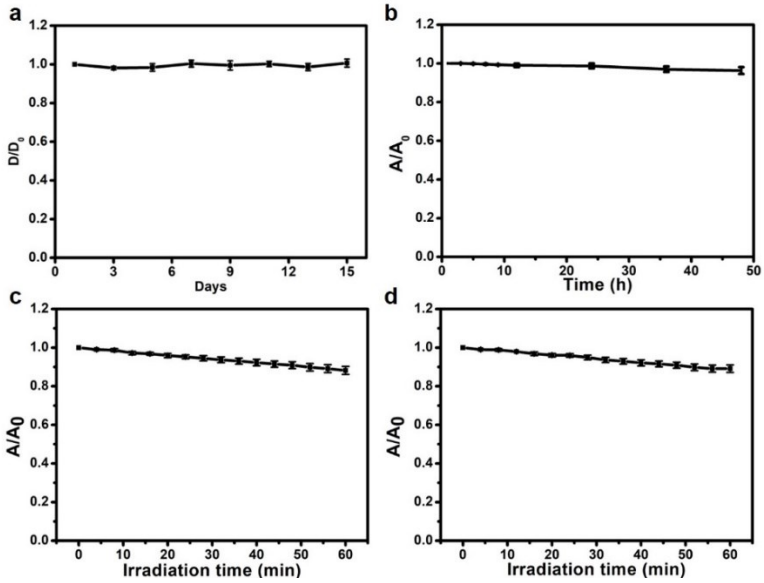

Fig. S5 (a) Hydrodynamic diameter of BIBCl-PAE NPs in PBS buffer in different days. (b) The A/A_0 (675 nm) of BIBCl-PAE NPs in fetal calf serum at different times. Photostability of (c) BIBCl-PAE NPs and (d) BIBSG generated by reaction with GSH under the illumination of a xenon lamp (test absorption intensity at 675 nm).

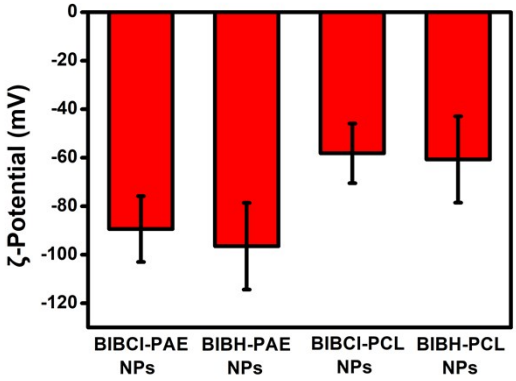

Fig. S6 Zeta-potential of the different polymeric micelles.

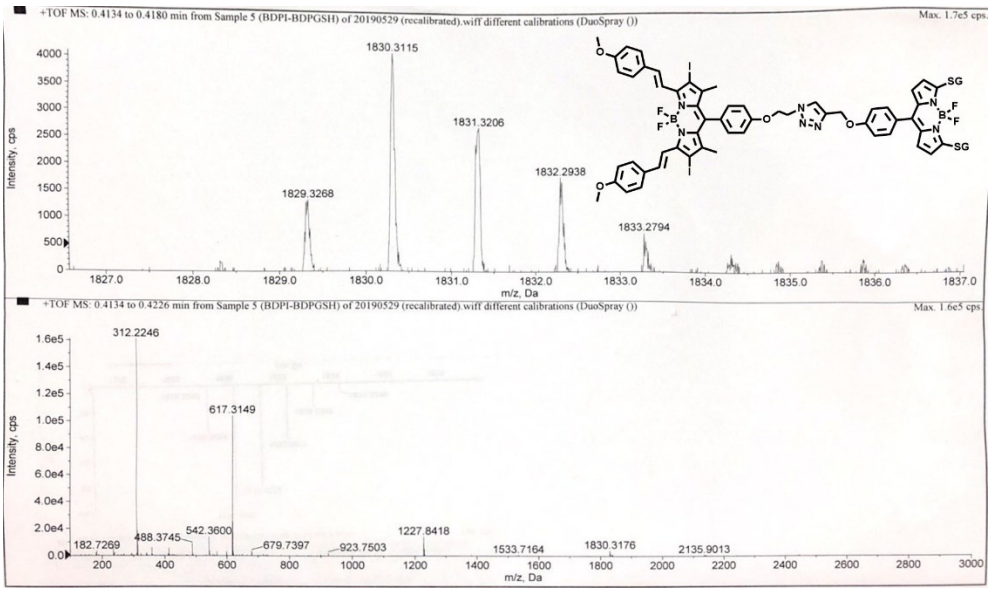

Fig. S7 The HRMS spectra of BIBSG.

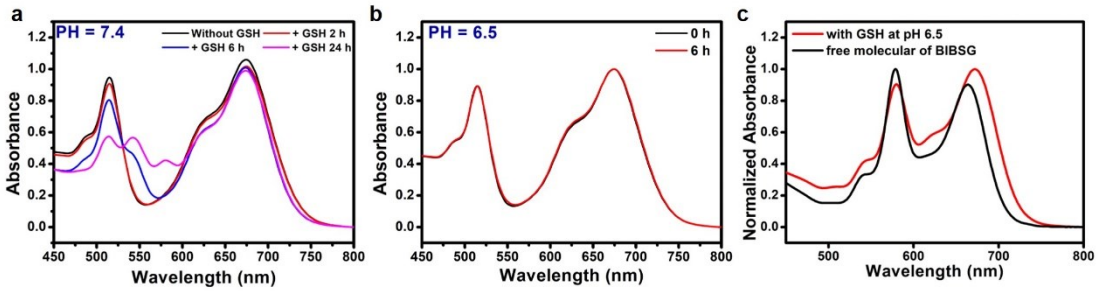

Fig. S8 (a) Time-dependent absorption spectra of BIBCl-PAE NPs (20 μM) with 50 equiv of GSH in PBS; (b) The absorption spectra of BIBCl-PAE NPs at PH 6.5 at different time points. (c) The normalized absorption spectra of GSH-treated BIBCl-PAE NPs at pH 6.5 and free BIBSG in MDSO.

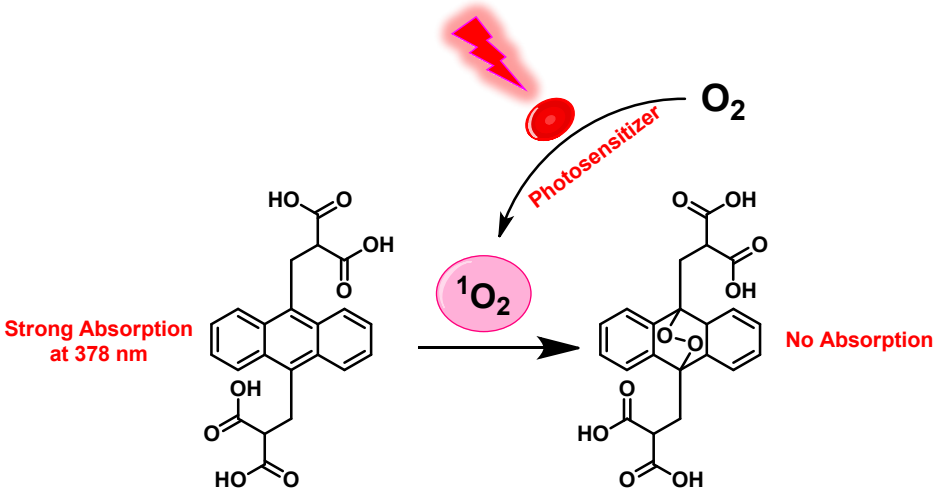

Fig. S9 The mechanism of 9,10-anthracenediyl-bis(methylene)-dimalonic acid (ABDA) as the $^1O_2$ scavenger monitors singlet oxygen generation in the solution.

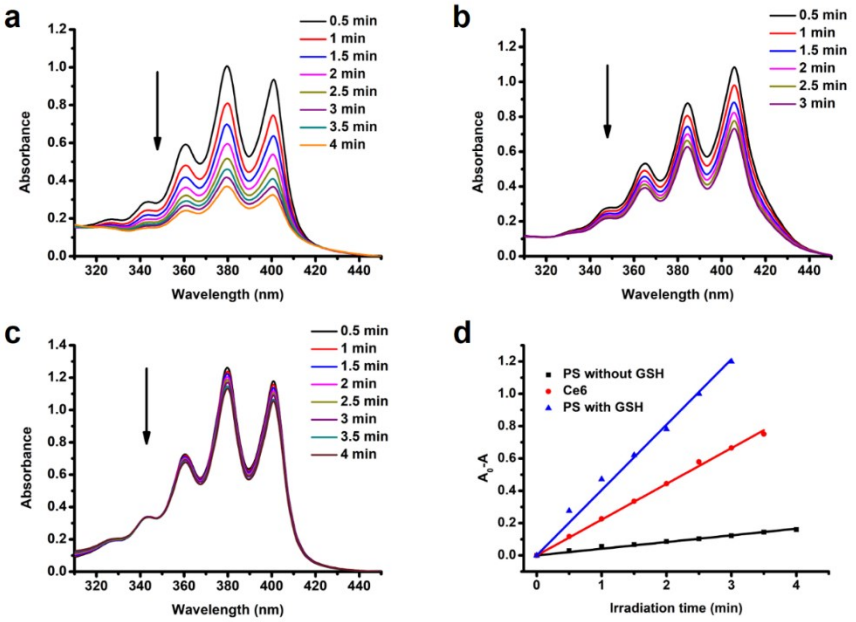

Fig. S10 Absorption spectra of ABDA at different time points in the presence of (a) BIBCl-PAE NPs with GSH, (b) Ce6 and (c) BIBCl-PAE NPs without GSH; (d) The absorbance changes of ABDA at 378 nm in the presence of different samples (white LED light irradiation, 400-800 nm, 10 mW cm^{-2}).

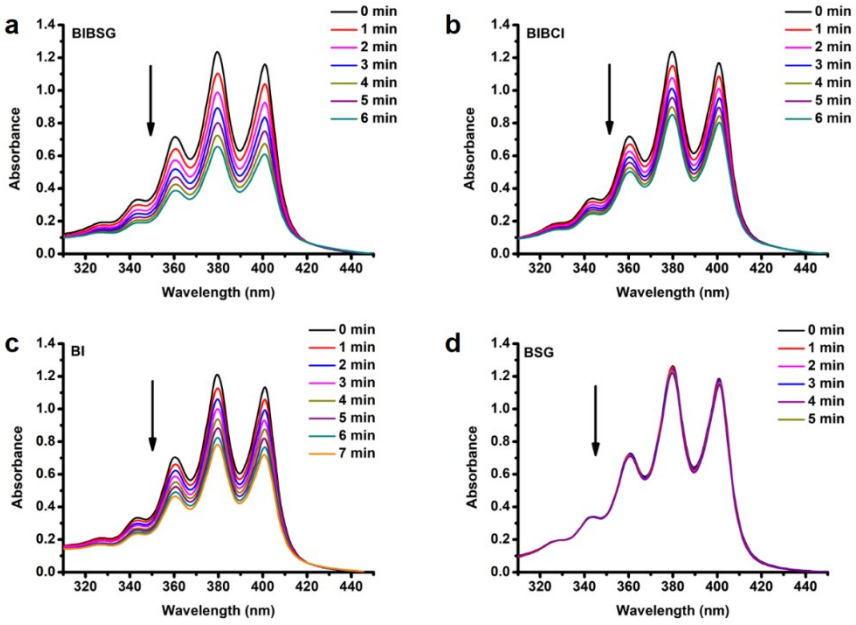

Fig. S11 Absorption spectra of ABDA at different time points in the presence of (a) BIBSG, (b) BIBCl (c) BI and (d) BSG in DMF (white LED light irradiation, 400-800 nm, 10 mW cm^{-2}).

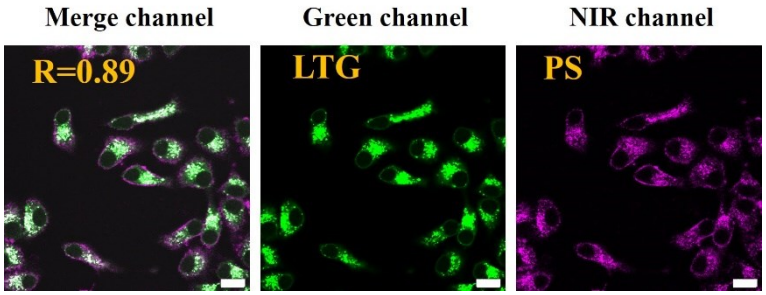

Fig. S12 Imaging of BIBCl-PAE NPs after 12 h incubation with LysoTracker Green (LTG) in HepG2 cells. R is the correlation coefficient. Scale bar, 20 μm.

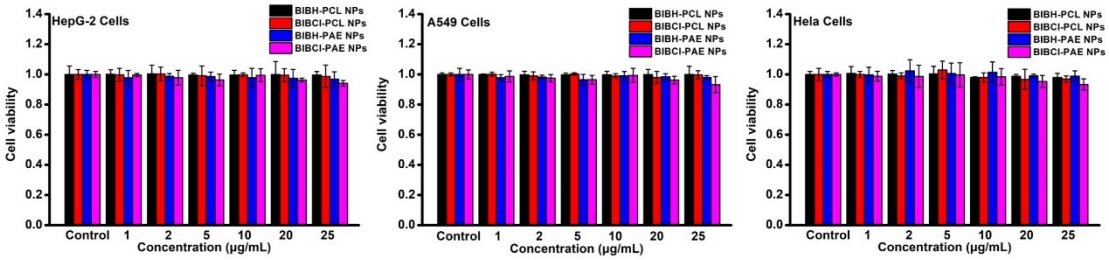

Fig. S13 Viability of various cancer cell lines (HepG2, A549, and Hela cells) after treatment at various doses of BIBH-PCL NPs, BIBCl-PCL NPs, BIBH-PAE NPs and BIBCl-PAE NPs without irradiation (incubated for 24 h), as measured by CCK-8 assay: (a) HepG2 cells; (b) A549 cells; (c) Hela cells.

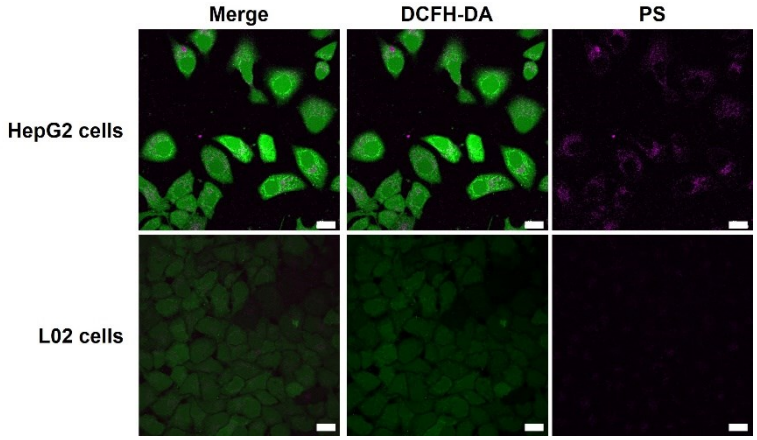

Fig. S14 Evaluation of ROS generation in HepG2 cells and L02 cells with DCFH-DA. Scale bar, 20 μm.

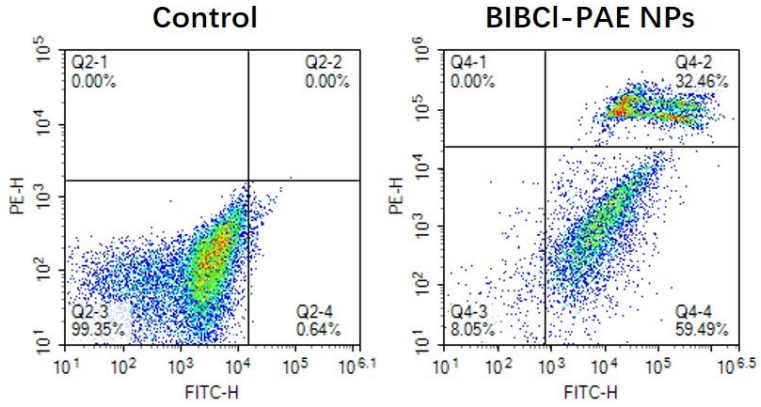

Fig. S15 Apoptosis analysis of HepG2 cells with BIBCl-PAE NPs.

4. Experimental data in vivo

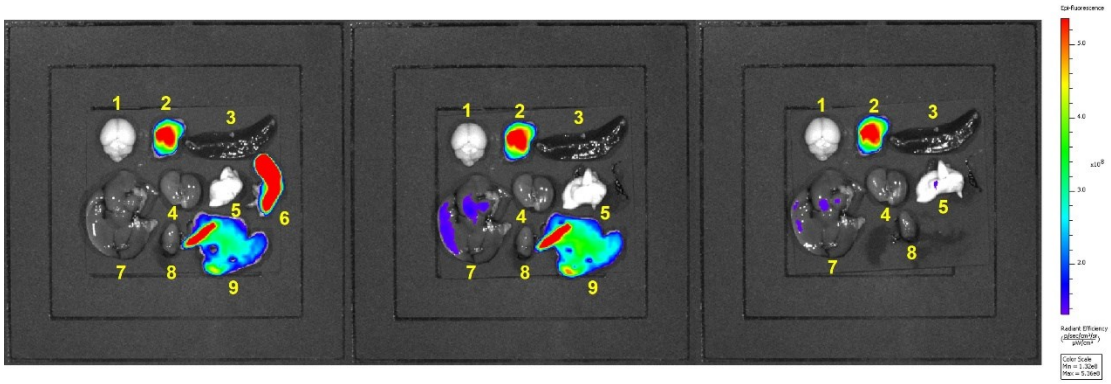

Fig. S16 Fluorescence images of ex-vivo organs harvested at 24 h postinjection (1. Brain; 2. Tumor; 3. Spleen; 4. Kidney; 5. Lung; 6. Stomach; 7. Liver; 8. Heart; 9. Intestines).

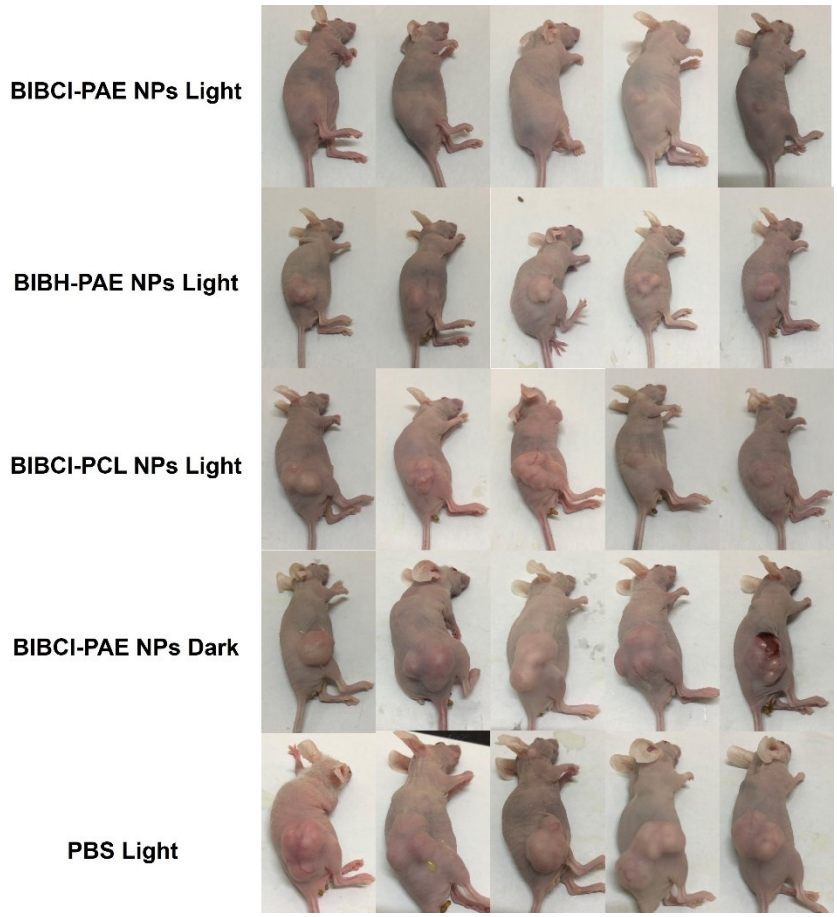

Fig. S17 Photos of mice bearing HepG2 tumor after relevant treatments.

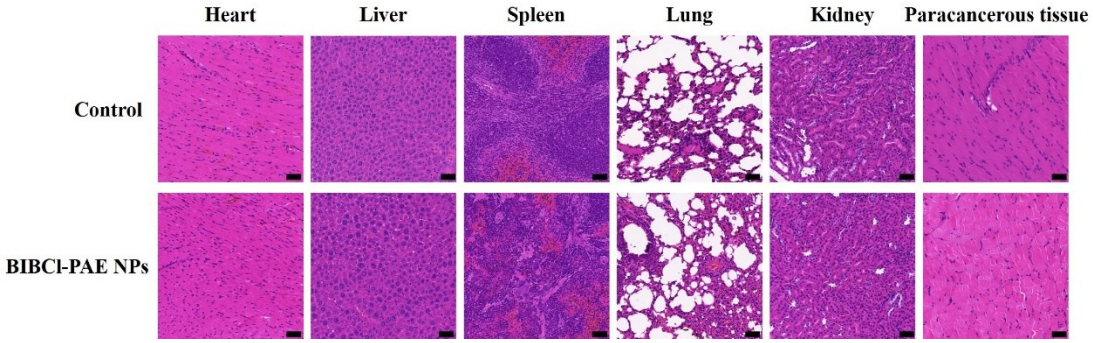

Fig. S18 Images of H&E stained sections of the paracancerous tissue and main tissues after various treatments, scale bar represents 50 μm.

5. NMR spectra and HRMS of the compounds

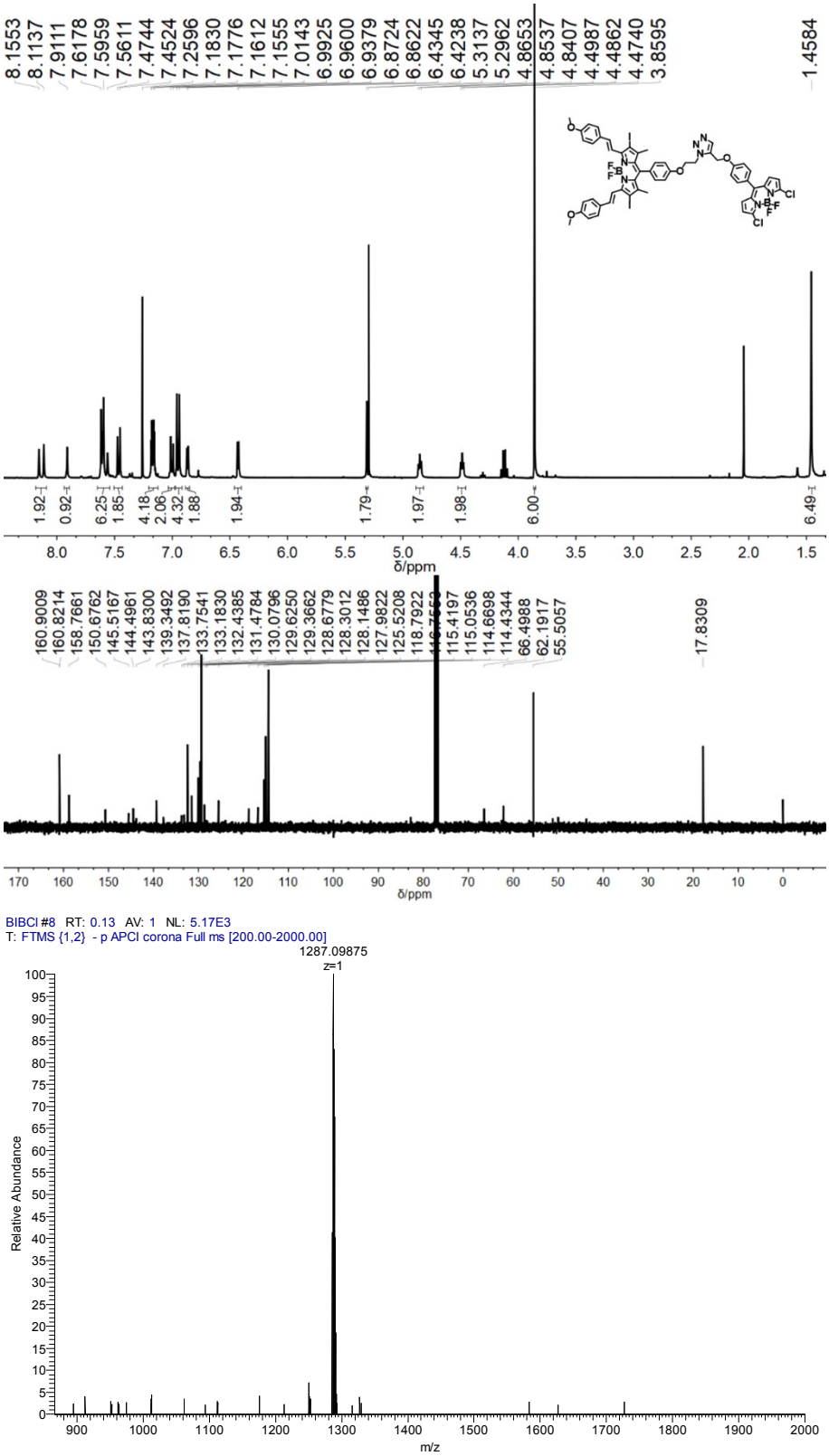

Fig. S19 ^{1}H-NMR and ^{13}C-NMR spectra in $CDCl_3$, as well as HRMS spectra of BIBCl.

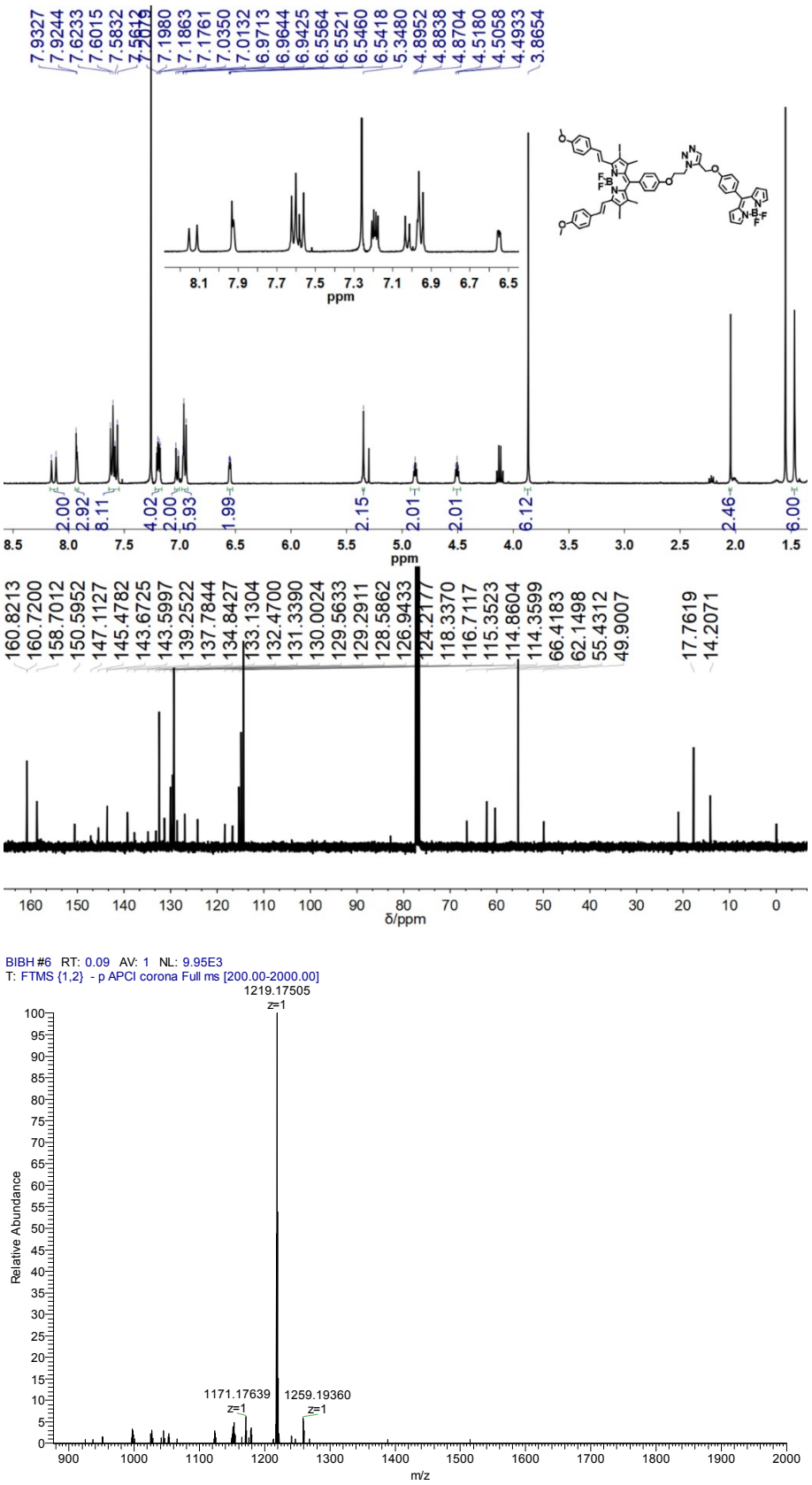

Fig. S20 ^{1}H-NMR and ^{13}C-NMR spectra in $CDCl_3$, as well as HRMS spectra of BIBH.

1. L. Huang, Z. Li, Y. Zhao, J. Yang, Y. Yang, A. I. Pendharkar, Y. Zhang, S. Kelmar, L. Chen, W. Wu, J. Zhao and G. Han, *Advanced Materials*, 2017, **29**, 1604789.